energy&fuels

Article

pubs.acs.org/EF

Assessing Biodegradation of Brazilian Crude Oils via Characteristic Profiles of O_1 and O_2 Compound Classes: Petroleomics by Negative-Ion Mode Electrospray Ionization Fourier Transform Ion Cyclotron Resonance Mass Spectrometry

Laercio L. Martins,*[,†] Marcos A. Pudenzi,[‡] Georgiana F. da Cruz,*[,†] Heliara D. L. Nascimento,[‡] and Marcos N. Eberlin[‡]

[†]Laboratory of Petroleum Engineering and Exploration (LENEP), North Fluminense State University (UENF), Macaé, Rio de Janeiro 27910-970, Brazil

[‡]ThoMSon Mass Spectrometry Laboratory, University of Campinas, Campinas, São Paulo 13083-970, Brazil

Supporting Information

ABSTRACT: Profiles for polar heteroatom compounds were obtained via Fourier transform ion cyclotron resonance mass spectrometry (FT-ICR MS) using electrospray ionization (ESI) in negative-ion mode for a set of 30 Brazilian oil samples from distinct sedimentary basins and used to estimate biodegradation extents. The samples were initially subjected to traditional geochemical biodegradation analysis to classify them in term of biodegradation levels as based on the Peters and Moldowan scale (PM scale). When the profiles were correlated with the PM scale, it was found that the O_1, N, NO_2, NO_3, and N_3O_2 classes decrease, whereas the O_2, O_3, and O_4 classes increase in relative abundance with biodegradation. The acyclic to cyclic acids (A/C) ratio of the O_2 class, mainly composed of naphthenic acids, provided a robust parameter to classify biodegradation levels of Brazilian oils. A modified saturated acid (SA) index was also used to classify biodegradation levels. For the O_1 class, two new monoaromatic (MA) indexes were proposed to predict the biodegradation extent. These MA parameters are based on the most readily degraded phenolic and/or benzylic O compounds by microorganisms and the persistence of O compounds with higher double bond equivalent (DBE) values in more degraded oils.

INTRODUCTION

Traditional analytical techniques, such as gas chromatography with flame ionization detector (GC−FID) and gas chromatography coupled to mass spectrometry (GC−MS), have been successfully used to analyze petroleum composition and make geochemical assessments of thermal maturity, related sources, biodegradation levels, and both oil−oil and source−oil correlations.[1−3] However, these techniques quantitatively determine only up to a few hundred components of the petroleum sample, normally saturated and aromatic hydrocarbons, sampling therefore only a tiny fraction of the diverse petroleum composition.[4] Fortunately, advances mainly in mass spectrometry (MS) and gas chromatography (GC) had led a much detailed access to petroleum composition at the molecular level.[4,5] For MS, Fourier transform ion cyclotron resonance mass spectrometry (FT-ICR MS) has offered ultrahigh resolution and mass accuracy, which facilitate formula attribution to thousands of the most polar components of such highly complex mixtures present in petroleum samples.[5−7]

Using ionization techniques, such as atmospheric pressure photoionization (APPI) and electrospray ionization (ESI), FT-ICR MS unequivocally identifies elemental compositions for resolved ions.[6,8,9] From these formulas, more polar petroleum components are classified according to their heteroatom class ($N_nO_oS_s$), double bond equivalent (DBE), and carbon number. On the basis of this fine "MS petroleomic" approach[6] and such detailed chemical composition parameters, properties and behaviors of petroleum samples are predicted.

FT-ICR MS petroleomics has been used in petroleum geochemistry in a wide variety of investigations, such as in studies of the oil maturity level,[10−12] measurements of the oil total acid number (TAN),[13,14] oil spill source identification,[15] and levels of oil biodegradation.[6,16−20] For biodegradation, the O classes have been found to be most reliable because they seem to be the most affected.[6,16−20]

Using ESI(−) FT-ICR MS data, Kim et al.[16] proposed the acyclic to 2−4 ring cyclic O_2 species (A/C) ratio as the best parameter to access biodegradation. Hughey et al.[17] also reported that biodegraded oils display increasing relative abundance for the O_2 class, with a decrease in the abundance of acyclic fatty acids relative to multi-ring naphthenic acids. Liao et al.[18] also found that the O_2 and N_1O_2 classes increase whereas the N_1 and N_1O_1 classes decrease with biodegradation. Vaz et al.[19] also observed that biodegradation leads to an increase in the abundance of saturated acids with a lower DBE, as demonstrated by an A/C ratio, and proposed a saturated acid (SA) index to access biodegradation. More recently, Angolini et al.[20] proposed a biodegradation scale using O_2 species based on the premise that compounds with less complex structures (a

Received: January 11, 2017
Revised: May 7, 2017
Published: June 21, 2017

DOI: 10.1021/acs.energyfuels.7b00109
Energy Fuels 2017, 31, 6649−6657

lower DBE) are more depleted than those with more complex structures (a higher DBE). Despite such studies, a generally accepted MS petroleomics parameter to access biodegradation seems to have not yet been established. FT-ICR MS data are highly diverse, and different types of information as summarized in diverse parameters can be extracted.[6] The great variety in petroleum composition around the world also claims for more systematic MS petroleomics studies regarding biodegradation prediction.

In this study, ESI(−) FT-ICR MS analyses was performed to a large set of 30 Brazilian non-genetically related crude oils with distinct levels of biodegradation as measured by traditional geochemical techniques and new MS petroleomics parameters to assess biodegradation were evaluated.

MATERIALS AND METHODS

Sample Set. A total of 30 oil samples were used, in which 25 samples were from five Brazilian basins and 5 samples were from unknown specific sources. These oil samples with their corresponding American Petroleum Institute (API) gravities were codified as show in Table 1. These five sedimentary basins are among the provinces that are currently responsible for the domestic oil production in Brazil.[21]

Specifically, samples C01−C18 were from the Campos Basin, the most explored and prolific Brazilian basin, producing nearly 60% of the Brazilian oil.[21,22] Sample SA01 was from the Santos Basin, the largest offshore basin and the second most prolific basin in Brazil, where the most productive field from the pre-salt layer, the Lula field, is located.[21] Samples R01−R04 were from the Recôncavo Basin, one of the onshore basins that sustained Brazil's production up to the end of the 1960s but is still underexplored.[21,23] Sample SO02 was from the Solimões Basin, with the largest proven reserves of natural gas and which produces the lightest oil in Brazil.[21,23] Sample P01 was from the Potiguar Basin, an on- and offshore basin, which has the region with the biggest onshore oil producer in Brazil.[21,23]

Table 1. Origin (Basin), Codes, and API Gravity for the 30 Brazilian Oil Samples

basin	sample	API gravity (deg)
Campos	C01	17
	C02	24
	C03	24
	C04	21
	C05	20
	C06	26
	C07	20
	C08	19
	C09	24
	C10	19
	C11	20
	C12	21
	C13	26
	C14	26
	C15	24
	C16	23
	C17	22
	C18	24
Santos	SA01	30
Recôncavo	R01	42
	R02	39
	R03	21
	R04	39
Solimões	SO02	43
Potiguar	P01	30
unknown	U01	33
	U03	21
	U04	22
	U05	23
	U06	38

GC−FID. Crude oil samples were subjected to GC−FID analysis using an Agilent 6890N gas chromatograph with a flame ionization detector (using synthetic air, H_2, and N_2) equipped with a HP-5 fused silica capillary column (30 m × 0.32 mm × 0.25 μm film thickness, Agilent, Santa Clara, CA, U.S.A.). The GC oven was isothermally held at 40 °C for 1 min and ramped from 40 to 310 °C at 6 °C min^{-1}, with the final temperature held for 19 min. The injector temperature was 290 °C, and the FID was set at 320 °C. Helium was used as the carrier gas, with a 2.2 mL min^{-1} constant flow. 5α-Androstane at a concentration of 0.02 mg mL^{-1} was used as an internal standard for the quantification of *n*-alkanes.

GC−MS. Analyses of the saturated and aromatic hydrocarbon fractions were conducted using an Agilent 6890N gas chromatograph, equipped with DB5MS (30 m × 0.25 mm × 0.25 μm film thickness) coupled to an Agilent 5973-MSD mass spectrometer. The GC oven for the saturated hydrocarbon analysis was isothermally held at 60 °C for 2 min, ramped from 60 to 200 °C at 22 °C min^{-1}, then isothermally held at 200 °C for 3 min, and finally ramped from 200 to 300 °C at 3 °C min^{-1}, with the final temperature held for 25 min. The GC oven for the aromatic hydrocarbon analysis was isothermally held at 70 °C for 1 min, ramped from 70 to 110 °C at 22 °C min^{-1}, then isothermally held at 110 °C for 1 min, ramped from 110 to 200 °C at 1.50 °C min^{-1}, then isothermally held at 200 °C for 1 min, and finally ramped from 200 to 300 °C at 3.00 °C min^{-1}, with the final temperature held for 10 min. Helium was used as the carrier gas, with a 1 mL min^{-1} constant flow. The injector and transfer line temperatures were 300 and 280 °C, respectively. MS was operated in the electron ionization (EI) mode with an ionization energy of 70 eV and a source temperature of 230 °C. Injection was performed in the splitless mode, with a volume of injection of 1 μL. Data were collected in selected ion monitoring (SIM) and full-scan modes.

ESI(−) FT-ICR MS. The samples (2 mg) were previously dissolved in 1 mL of toluene and then diluted with 1 mL of methanol, containing 0.2% ammonium hydroxide. Solvents were of high-performance liquid chromatography (HPLC) grade, purchased from Sigma-Aldrich, and used as received. Direct infusion ESI(−)−MS in the negative-ion mode was performed, and samples were analyzed by a 7.2 T LTQ FT Ultra mass spectrometer (ThermoScientific, Bremen, Germany) with a resolving power of 400 000 on the 200−1000 Da mass range. A 5 μL min^{-1} syringe flow was used, with a spray voltage of 3.1 kV, and a 100 scans spectrum was acquired for each sample.

Data Processing. FT-ICR MS data were processed using a custom algorithm developed specially for petroleum data processing: the PetroMS software.[24] This software was designed for formula attribution and recalibration for a known homologous series (O_2 class) from the measured *m*/*z* values of polar crude oil compounds. For each spectrum, automated processing was performed to assign formulas to ion peaks with a signal-to-noise ratio of >3. Allowed elements were ^{12}C, ^{13}C, ^{1}H, ^{16}O, ^{14}N, and ^{32}S. The maximum allowed formula error was 1 ppm.

RESULTS AND DISCUSSION

Traditional Geochemical Analysis. Hydrocarbon analyses by GC−FID and biomarker analyses by GC−MS were conducted to assess the biodegradation degree of the oil samples by these most conventional techniques. On the basis of the GC−FID and GC−MS data, the oil samples were classified in five levels of biodegradation according to the Peters and Moldowan scale (PM scale):[2] PM level 0−1 (non-/very slight), PM level 2−3 (slight/moderate), PM level 3 (moderate), PM level 4−5 (heavy), and PM level 5−10 (heavy/severe). Table 2 shows the quantitative parameters obtained for our set of 30 oil samples.

DOI: 10.1021/acs.energyfuels.7b00109
Energy Fuels 2017, 31, 6649−6657

Table 2. Bulk Geochemical Parameters for the Oil Samples Classified in Five Levels of Biodegradation According to the PM Scale[2]

		GC−FID				GC−MS					
sample	level of biodegradation[a]	*n*-alkanes (mg/100 of mg of oil)[b]	*n*-alkanes	Pr/*n*-C_{17}[c]	Ph/*n*-C_{18}[d]	H_{30}/AC[e]	H_{30}/Ph[f]	25NH/H_{30}[g]	TA/P[h]	TA/MDB[i]	TA/CHR[j]
R01	0−1	11.34	C_{13}−C_{38}	0.28	0.20	0.00	0.10	nd[k]	nd	nd	nd
R02		14.91	C_{13}−C_{38}	0.26	0.17	0.01	0.20	nd	0.03	0.16	0.16
R04		13.57	C_{13}−C_{39}	0.25	0.17	0.01	0.29	nd	0.02	0.14	0.12
SO02		3.70	C_{13}−C_{35}	0.14	0.06	nd	nd	nd	nd	nd	nd
U06		4.52	C_{13}−C_{38}	0.32	0.21	0.00	0.19	nd	0.00	0.00	0.05
SA01	2−3	2.33	C_{13}−C_{35}	0.96	0.66	0.06	0.73	0.04	0.04	0.17	0.43
P01		6.70	C_{13}−C_{36}	0.90	0.33	0.06	0.79	nd	0.07	0.64	0.47
U01		3.06	C_{13}−C_{37}	0.79	0.58	0.02	0.38	nd	0.18	0.54	2.16
C01	3	1.23	C_{13}−C_{35}	0.74	0.56	0.07	2.78	0.07	0.07	0.15	0.48
C02		1.45	C_{13}−C_{35}	0.75	0.56	0.06	3.03	0.01	0.05	0.11	0.42
C03		1.78	C_{13}−C_{35}	0.95	0.64	0.06	2.60	0.01	0.05	0.11	0.45
C04		1.54	C_{13}−C_{35}	0.85	0.64	0.07	3.18	0.10	0.12	0.32	0.94
C06		1.51	C_{13}−C_{33}	0.97	0.66	0.07	2.81	0.01	0.05	0.12	0.41
C07		1.10	C_{13}−C_{34}	0.81	0.61	0.10	4.14	0.03	0.09	0.20	0.62
C09		2.21	C_{13}−C_{35}	0.77	0.58	0.05	2.05	0.04	0.04	0.11	0.39
C11		2.33	C_{13}−C_{35}	0.88	0.69	0.07	2.75	0.07	0.10	0.30	0.78
C12		0.97	C_{13}−C_{35}	1.50	1.08	0.08	3.15	0.01	0.05	0.10	0.48
C13		1.53	C_{13}−C_{35}	0.76	0.55	0.08	3.38	0.01	0.03	0.09	0.27
C14		1.72	C_{13}−C_{35}	0.94	0.65	0.06	2.52	0.05	0.05	0.10	0.49
C15		1.11	C_{13}−C_{36}	0.95	0.65	0.06	2.56	0.06	0.04	0.10	0.39
C16		1.26	C_{13}−C_{35}	0.86	0.61	0.08	3.41	0.06	0.04	0.11	0.38
C17		0.91	C_{13}−C_{34}	0.81	0.60	0.10	4.83	0.08	0.06	0.13	0.47
C18		2.62	C_{13}−C_{36}	1.94	0.71	0.08	2.88	0.04	0.17	0.79	1.40
C05		0.36	C_{13}−C_{29}	1.25	0.91	0.16	8.14	0.01	0.05	0.14	0.43
C08	4−5	0.13	C_{13}−C_{23}	6.48	6.45	0.14	3.10	0.03	0.10	0.23	0.84
C10		0.35	C_{13}−C_{29}	1.41	0.96	0.25	9.29	0.03	0.04	0.21	0.39
U03		0.35	C_{13}−C_{27}	5.46	3.77	0.21	1.17	0.04	0.06	0.17	0.60
U04		0.54	C_{13}−C_{30}	3.54	2.44	0.12	1.06	0.02	0.06	0.16	0.62
U05		0.90	C_{13}−C_{33}	2.29	1.55	0.17	1.07	0.03	0.07	0.16	1.40
R03	5−10	0.22	C_{13}−C_{34}	nd	0.58	0.49	72.40	nd	1.20	1.11	0.92

[a]Level of biodegradation according to the PM scale. [b]Calculated from peak areas of $\sum C_{13}$−C_{39} *n*-alkanes in whole oil chromatograms, using 5α-androstane (0.02 mg mL^{-1}) as the internal standard. [c]Calculated from the peak area of pristane over the peak area of C_{17} *n*-alkane in the whole oil chromatograms. [d]Calculated from the peak area of phytane over the peak area of C_{18} *n*-alkane in the whole oil chromatograms. [e]Calculated from the peak area of H_{30} 17α(*H*),21β(*H*)-hopane in the *m*/*z* 191 chromatogram over the peak area of alkylcyclohexanes in the *m*/*z* 83 chromatogram. [f]Calculated from the peak area of H_{30} 17α(*H*),21β(*H*)-hopane in the *m*/*z* 191 chromatogram over the peak area of phytane in the *m*/*z* 183 chromatogram. [g]Calculated from the peak area of H_{29} 17α(*H*),21β(*H*)-25-*nor*-hopane over the peak area of 17α(*H*),21β(*H*)-hopane in the *m*/*z* 191 chromatogram. [h]Calculated from the peak area of triaromatic steroids in the *m*/*z* 231 chromatogram over the peak area of phenanthrene in the *m*/*z* 178 chromatogram. [i]Calculated from the peak area of triaromatic steroids in the *m*/*z* 231 chromatogram over the peak area of methyldibenzothiophenes in the *m*/*z* 198 chromatogram. [j]Calculated from the peak area of triaromatic steroids in the *m*/*z* 231 chromatogram over the peak area of chrysene in the *m*/*z* 228 chromatogram. [k]nd = not detected.

On the basis of the GC−FID hydrocarbon analyses, the biodegradation extent of oil samples was estimated, where *n*-alkane concentrations are known to diminish with rising biodegradation (Table 2). Note that concentrations on average of 9.60 mg/100 mg of oil to non-/very slight degraded samples (PM level 0−1) reach 0.42 mg/100 mg of oil to heavy/severe degraded samples (PM level 4−10). The Pr/*n*-C_{17} and Ph/*n*-C_{18} ratios also increased with increasing biodegradation levels (Table 2) as a result of an expected biodegradation trend, because the isoprenoid alkanes, such as pristane (Pr) and phytane (Ph), are known to be more resistant to biodegradation than linear alkanes (*n*-alkanes) with similar physical and chemical properties.[25] Figure 1 shows examples of whole oil gas chromatograms obtained by GC−FID for each level of biodegradation identified (the chromatograms of the other samples are shown in Figures S1 and S2 of the Supporting Information), which also reveal an increase of intensity of peaks in the unresolved complex mixture (UCM) region with increasing biodegradation, with results in humps in the gas chromatograms.[25]

As is traditionally performed in petroleum geochemistry, the biodegradation levels of oil samples were also estimated via GC−MS biomarker analyses, using parameters based on relative abundance of compound classes and qualitative biodegradation scales (Table 2).[3,26,27] According to the classical PM scale,[2] biodegradation generally more promptly removes components from petroleum samples in the following order: *n*-alkanes > alkylcyclohexanes > acyclic isoprenoids > bicyclic alkanes > steranes > hopanes.[3]

Figures S3−S5 of the Supporting Information (mass chromatograms for *m*/*z* 81) show that alkylcyclohexanes were detected in all oil samples, with a distribution similar to the *n*-alkane profile. These compounds have already been detected in Brazilian oils from Campos,[22] Sergipe-Alagoas,[28] and Potiguar Basins.[29] These hydrocarbons were shown to be useful to predict biodegradation, because they begin to be

DOI: 10.1021/acs.energyfuels.7b00109
Energy Fuels 2017, 31, 6649−6657

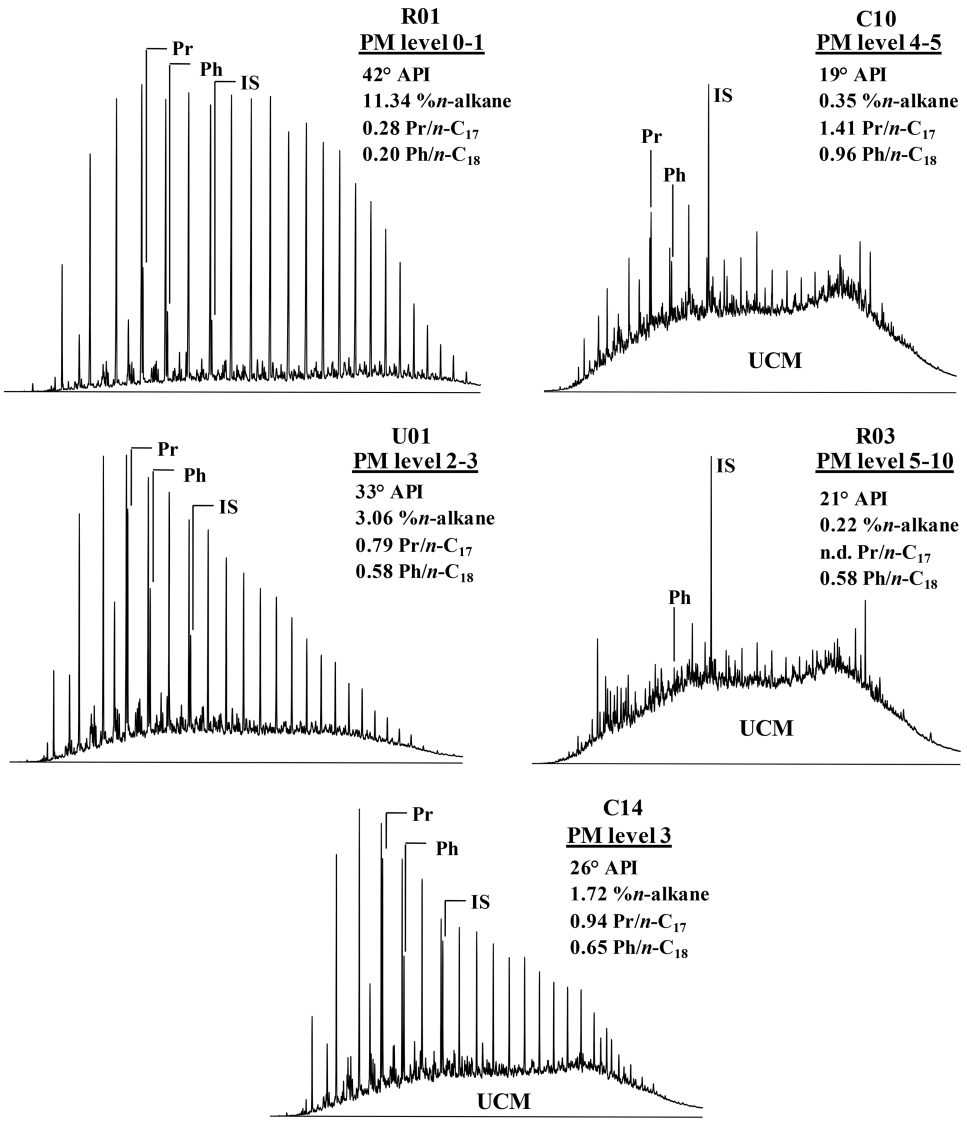

Figure 1. Typical whole oil gas chromatograms of samples that differ in degree of biodegradation, according to the PM scale.[2] Peaks marked IS refer to the internal standard (5α-androstane). Pr, pristane; Ph, phytane.

degraded at moderate levels of biodegradation, and at heavy biodegradation levels, they had an intermediate alteration, reaching a complete removal at severe levels of microbial degradation.[2,22] Figure S3 of the Supporting Information of selected mass chromatograms (m/z 81) for oil samples with a distinct level of biodegradation shows indeed a decrease in alkylcyclohexane abundances with increasing biodegradation, reaching very low abundances for sample R03, which has the highest level of biodegradation. The H_{30}/AC ratio, that is, the H_{30} 17α(*H*),21β(*H*)-hopane to the sum of alkylcyclohexanes ratio, also shows the same tendency (Table 2), with lower values for least biodegraded oil samples (PM level 0−1). H_{30} is considered in the H_{30}/AC ratio because this biomarker is very resistant to biodegradation.

Other biomarkers were also monitored to evaluate biodegradation based on the PM scale.[2,3] For instance, the 17α(*H*),21β(*H*)-hopane (H_{30}) and triaromatic sterane (TA) levels remained unchanged, because none of the studied oil samples displays a severe level of biodegradation (except sample R03). The isoprenoids (C_{15}−C_{35}, such as phytane), phenantrene (P), methyldibenzotiophene (MDB), and chrysene (CHR) indeed decreased in abundances at moderate biodegradation levels, with intermediate degradation at heavy levels and complete removal at severe biodegradation levels. On the basis of these trends (Table 2), the following ratios were used: H_{30} 17α(*H*),21β(*H*)-hopane to phytane (H_{30}/Ph) and triaromatic sterane to phenanthrene (TA/P), methyldibenzothiophene (TA/MDB), and chrysene (TA/CHR).

To verify whether samples could be mixtures of oils with different levels of biodegradation, the presence of H_{30} 17α(*H*),21β(*H*)-25-*nor*-hopane (25NH) was monitored. It is known that advanced levels of microbial degradation lead to demethylation of H_{30} 17α(*H*),21β(*H*)-hopane (shown by the 25NH/H_{30} ratio; Table 2).[25] The failure to detect 25NH in the non- to slight biodegraded samples (except to sample SA01 but at a low value) and the low values of 25NH in the moderate and heavy biodegraded samples corroborate against mixtures. In sample R03, 25NH was not detected probably as a result of its very extensive biodegradation.[2]

Petroleomics Analysis. It is known that biodegradation changes the distribution of saturated and aromatic hydrocarbons by selective removal, because this trend is well-

DOI: 10.1021/acs.energyfuels.7b00109
Energy Fuels 2017, 31, 6649−6657

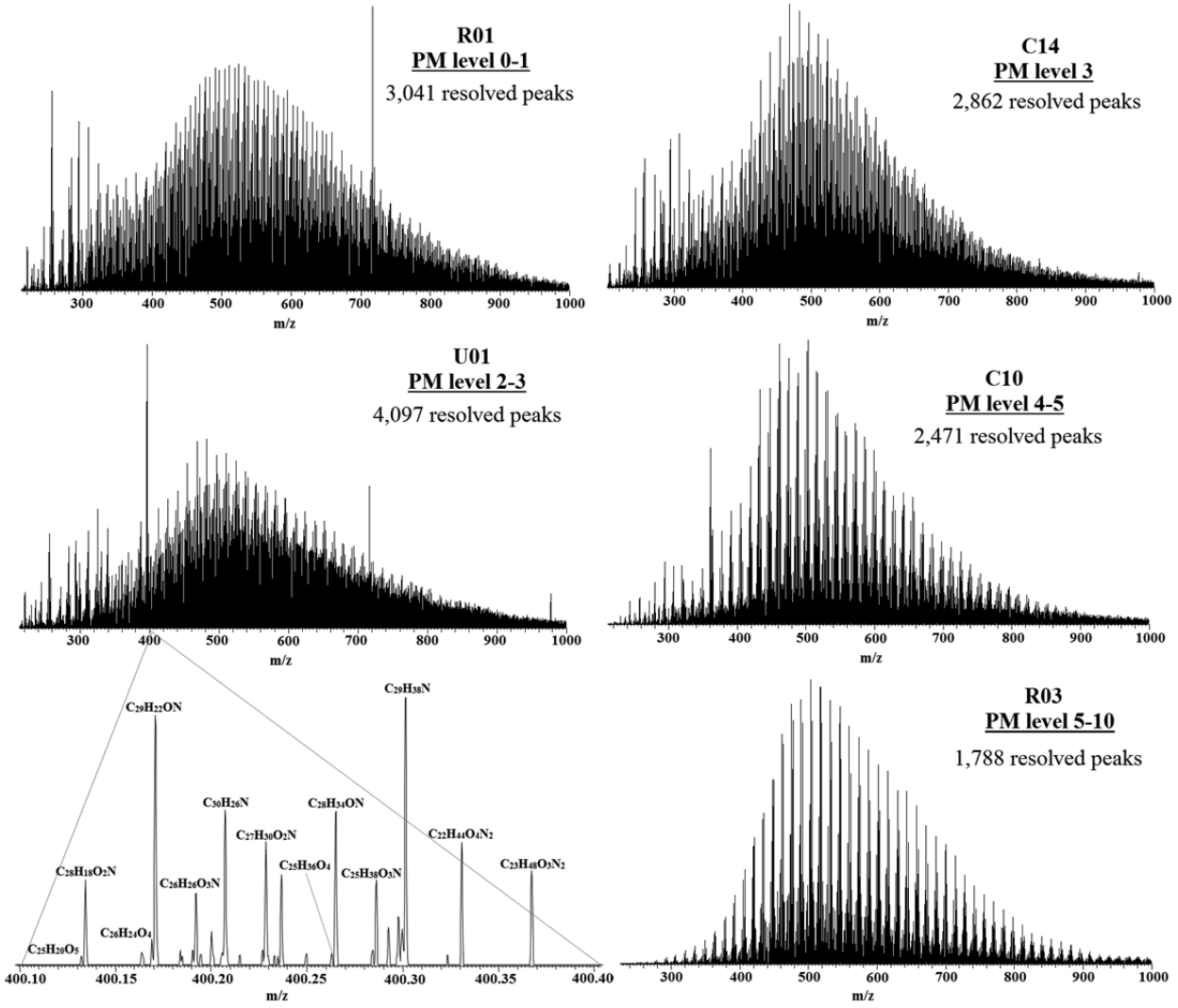

Figure 2. Broadband ESI(−) FT-ICR mass spectra of typical oil samples, with their number of assigned peaks, and the scale-expanded segment of the mass spectrum from m/z 400.10 to 400.40 for sample U01.

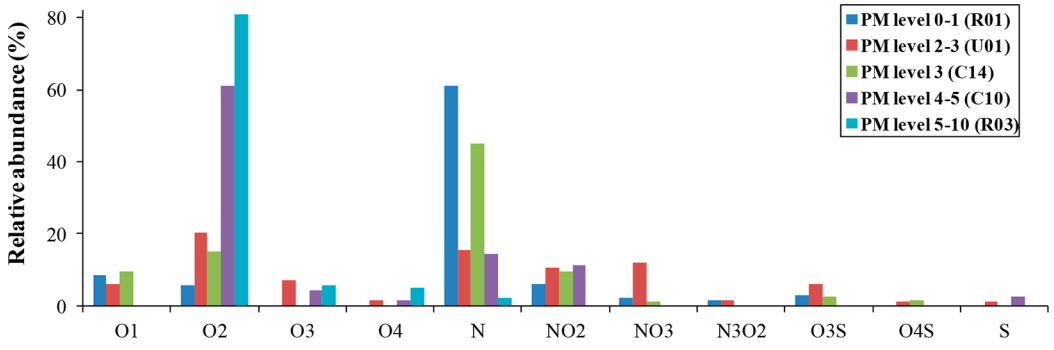

Figure 3. Relative abundances of polar heteroatom classes as measured by the ESI(−) FT-ICR MS data. Note the strongest correlation with biodegradation for the O_2 class.

consolidated in petroleum geochemistry,[1] and their analysis via GC is a well-established parameter to assess biodegradation.[3,26,27,30,31] However, concomitantly, biodegradation also alters the profiles of polar compounds, indicating that FT-ICR MS data can also be used to obtain parameters to assess biodegradation.[6,16]

Figure 2 shows typical broadband ESI(−) FT-ICR mass spectra obtained for the oil samples (R01, U01, C14, C10, and R03) with most contrasting biodegradation levels (the spectra for the other oil samples are shown in Figures S6 and S7 of the Supporting Information). For sample U01, a scale-expanded segment of the data is shown to demonstrate data complexity and the separation power of the technique. Note that spectra for the most biodegraded oil samples (R03 and C10) contain less assigned ion peaks likely as a result of the selective removal of heteroatom compounds. According to Liao et al.,[18] reduction

DOI: 10.1021/acs.energyfuels.7b00109
Energy Fuels 2017, 31, 6649−6657

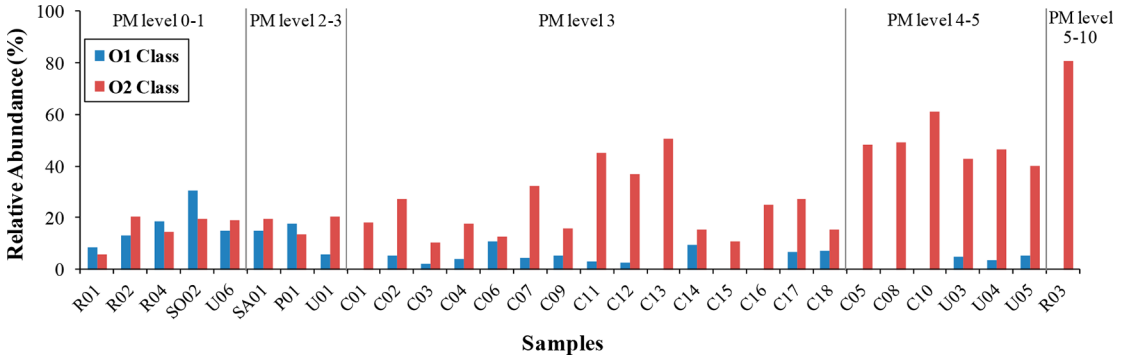

Figure 4. Relative abundance of O_1 and O_2 classes as a function of PM levels for all 30 Brazilian oil samples. Note a clear biodegradation trend, with enrichment of the O_2 class and the diminishing of the O_1 class.

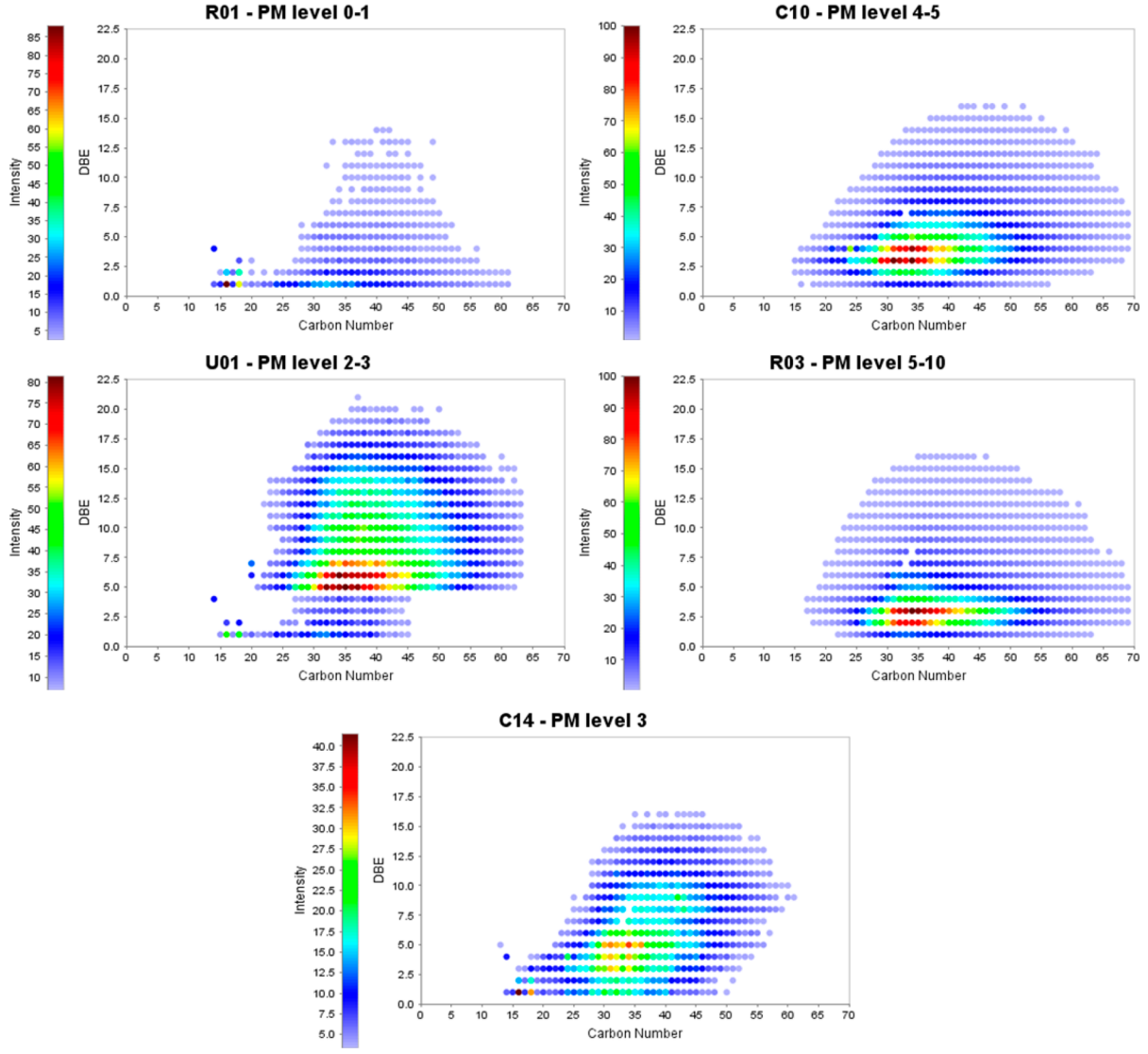

Figure 5. Isoabundance contoured plots of DBE versus carbon number for the O_2 class.

of ion peaks with increasing biodegradation could be related to the formation of compounds with reduced ionization efficiencies.

Heteroatom Class Distributions. Figure 3 now shows heteroatom class distributions to oil samples R01, U01, C14, C10, and R03. In general, a clear trend with respect to biodegradation is not observed at all, except for the O_2 class and less pronouncedly for the O_1 class. Indeed, it has been found that O classes are more affected by microbial degradation.[6] Vaz et al.[19] have also observed higher relative abundances for the O_2, O_3, and O_4 classes and lower relative abundances for the O_1 class as a function of increased biodegradation. However, in contrast, Angolini et al.[20] have

DOI: 10.1021/acs.energyfuels.7b00109
Energy Fuels 2017, 31, 6649−6657

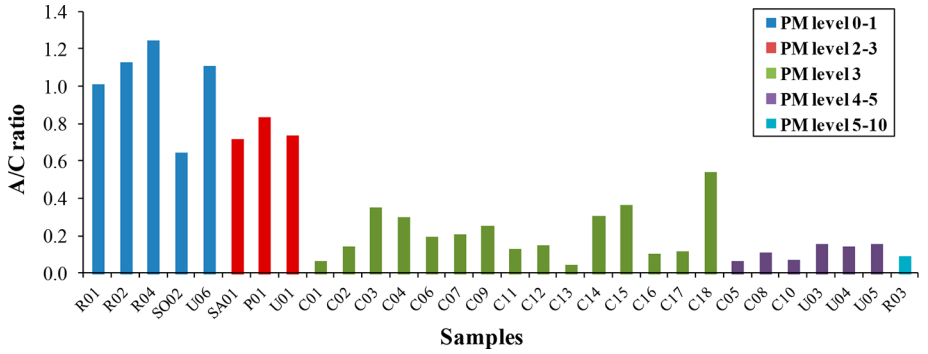

Figure 6. A/C ratios for the Brazilian non-genetically related oil samples.

reported higher abundances for the O_1 class with rising biodegradation.

Because the main changes occur in O_2 and O_1 classes (greatly depressed herein at higher biodegradation levels), we focused our evaluation on these diagnostic classes. Figure 4 shows the relative abundance of O_1 and O_2 classes for all Brazilian oil samples assessed. Note in Figure 4 that, indeed, generally the O_2 class increases and the O_1 class decreases with increasing biodegradation. Previous studies have shown that O_2 compound abundances increase with increasing biodegradation, because O_2 carboxylic acids are intermediates during the aerobic and anaerobic metabolisms of petroleum hydrocarbons.[17,19,32] In fact, biodegradation is the main process believed to form the high concentrations of naphthenic acids (O_2 compounds) found in crude oils.

Figures 3 and 4 show that there is a general trend associated with the O_1 and O_2 classes, but it seems inadequate to use relative abundances, as already discussed by Vaz et al.[19] For instance, C03 and C06 oil samples with a moderate degree of biodegradation (PM level 3) present lower O_2 class abundance than U01, R02, SO02, and U06 with non-/very slight degree of biodegradation (PM level 0−1). On the other hand, the C06 and C14 oil samples also present a moderate degree of biodegradation but present a higher O_1 class abundance than the R01 and U01 oil samples, belonging to non-/very slight and slight/moderate degree of biodegradation level groups, respectively. These results are in disagreement with the more general tendency of biodegradation (increasing O_2 class and decreasing O_1 class). Therefore, a thorough study of the type of compounds present in such O_1 and O_2 classes are necessary to develop a parameter that could better classify oil samples as a function of biodegradation levels using ESI(−) FT-ICR MS data.[19]

O_2 Class. The O_2 class is mainly composed of naphthenic carboxylic acids, a major product of biodegradation.[6] Figure 5 shows isoabundance contoured plots of DBE versus carbon number for samples R01, U01, C14, C10, and R03. Such a plot shows very distinct trends as a function of biodegradation. The R01 oil sample with a PM level of 0−1 displays much higher abundances at DBE of 1 as a result of saturated fatty acids and/or isoprenoid acids. However, the much more biodegraded C10 and R03 oil samples with PM levels of 4−5 and 5−10, respectively, display much higher abundances at DBE of 2, 3, and 4, in agreement with biodegradation being as effective to acids as for hydrocarbons, with bioresistance increasing with DBE (higher ring number and aromaticity), with acyclic acids with the greatest susceptibility to biodegradation.[16,32,33]

An interesting correlation was observed between the O_2 class distribution of Figure 5 and the hydrocarbon composition revealed by GC−MS (Table 2, Figure 1, and Figure S3 of the Supporting Information).[20] With the depletion of *n*-alkanes (Figure 1) as a result of biodegradation, there is an increase in the relative abundance of compounds with DBE of 1 until the PM level of 3. However, the relative abundance of DBE of 1 diminishes at heavy biodegradation levels (PM levels 4−5 and 6−10 in Figure 5) as a result of the preferred biodegradation of such acyclic acids. The increase in the relative abundance of DBE of 2 mainly as a result of monocyclic acids with biodegradation also correlates with the decrease of alkylcyclohexanes (Figure S3 of the Supporting Information), a possible precursor of monocyclic acids in the neutral fraction.[20] As showed by Angolini et al.,[20] compounds with DBE of 3, 4, 5, and 6 also have the same biodegradation trend; however, this correlation is difficult to interpret as a result of the complexity of biodegradation pathways.[34]

Using ESI FT-ICR MS data, Kim et al.[16] have suggested a biodegradation index to estimate the level of biodegradation based on the ratio of acyclic to cyclic naphthenic acids (A/C), as calculated by the ratio for DBE of 1/DBE of 2−4. They used the A/C ratio to measure a consistent decrease in acyclic acid and an increase in cyclic acid with biodegradation. The A/C ratio has successfully been used to monitor biodegradation of a single oil or a suite of genetically related oils.[17,19,20] We, therefore, tested the robustness of the A/C parameter to assess biodegradation of our suite of non-genetically related Brazilian oils (Figure 6). Note that, indeed, a trend of A/C decreasing with increasing biodegradation was observed. Therefore, the A/C ratio seems to offer a suitable parameter to assess biodegradation, even for non-genetically related oils.

Vaz et al.[19] have also suggested an slightly modified A/C ratio to assess biodegradation, which also takes four- and five-ring naphthenic acids into account by calculating the ratio between DBE of 1 and DBE of 2−6, coupled to a new parameter called the SA index, which is calculated by the sum of the relative abundance of DBE of 1−6 for the O_2 class. However, as Figure 7a shows, the SA index was shown to be unreliable to assess biodegradation of the oil samples tested herein. This failure for the SA index is probably associated with the DBE of 1 (acyclic acid) components, whose relative abundance actually decreases with biodegradation as a result of their high susceptibility to microbial degradation.[16] We have, therefore, tested a modified SA index, using only the sum of relative abundance of DBE of 2−6 for the O_2 class (Figure 7b). Indeed, when DBE of 1 is eliminated, the modified SA index

DOI: 10.1021/acs.energyfuels.7b00109
Energy Fuels 2017, 31, 6649−6657

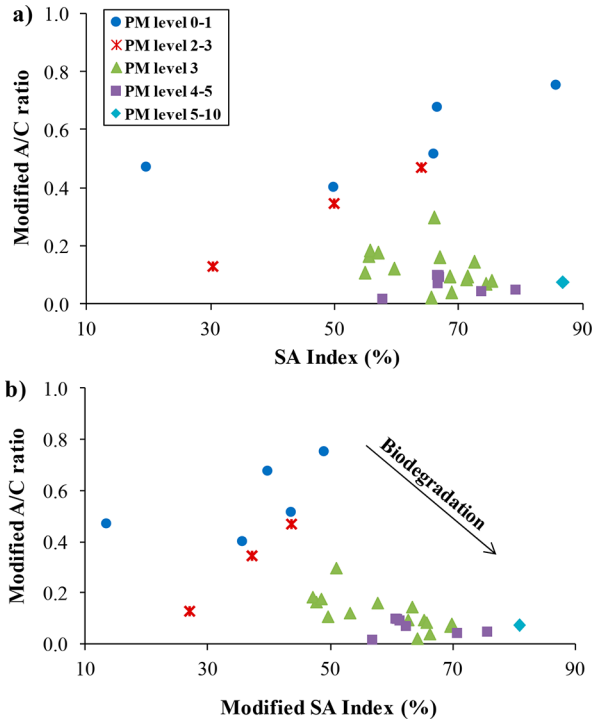

Figure 7. (a) Modified A/C ratio coupled to the SA index to assess biodegradation, as proposed by Vaz et al.[19] (b) Modified A/C ratio coupled to a modified SA index to assess biodegradation, proposed herein.

gives a much better prediction of biodegradation levels (Figure 7b).

O_1 Class. Such a class has been much less used than the O_2 class to assess biodegradation, but the O_1 class should provide important information concerning microbial degradation of crude oils. These O_1 species are most likely compounds with a hydroxyl functional group able to be deprotonated,[12] and according to Kim et al.,[16] they are more abundant in non-degraded oils and are at their maximum at DBE of 4 probably as a result of the formation of phenols and/or aromatic alcohols. Figure 4 clearly reflects such a behavior because less biodegraded oil samples presented the highest O_1 relative abundances, but such a class is rapidly consumed as biodegradation progresses.

The distribution of O_1 species presented in general a higher abundance to O compounds with DBE of 4 or 5 (Figure S8 of the Supporting Information). The abundance decreases with increasing DBE, with compounds detected up to DBE of 16. Of note, non-aromatic compounds (with DBE of 1−3) are absent in all oil samples, in which the behavior is expect in mature oils, as shown by Oldenburg et al.,[12] probably as a result of the thermal decomposition of these non-aromatic species prior to migration. To better highlight O_1 class variations with biodegradation, the distribution of DBE relative abundance for O_1 class is shown in Figure S9 of the Supporting Information for the following samples: R01 and R02 (PM level 0−1), SA01 and U01 (PM level 2−3), and C07 and C14. The biodegradation trends can be observed, in which DBE of 4 (monoaromatic core compounds) is the most abundant to non-/slightly biodegraded oil samples. However, in moderately biodegraded (PM level 3) oil samples, DBE of 5 is the DBE class most abundant.

Despite the robustness of the A/C ratio calculated from the O_2 class,[16] we have also tested two new parameters using O_1 heteroatom class to assess biodegradation, that is, two monoaromatic (MA) indexes 1 and 2, calculated by the ratio between DBE of 4 over DBE of 5 (MA1) or DBE of 7 (MA2) for the O_1 class tested (Figure 8). Indeed, both MA1 and MA2

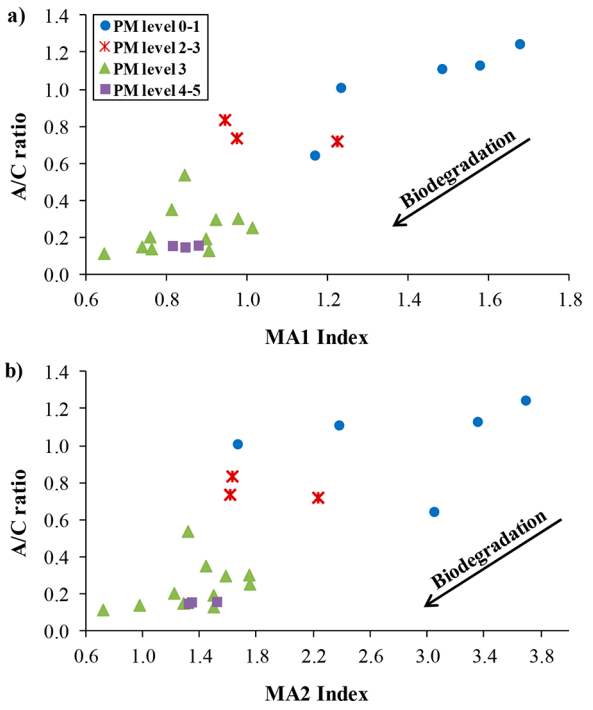

Figure 8. A/C ratio versus new proposed parameters (a) MA1 and (b) MA2 used to assess biodegradation via the O_1 class.

versus A/C decreased with increasing biodegradation, because phenolic and/or benzylic compounds with DBE of 4 are more readily degraded by microorganisms. According to Kim et al.,[16] DBE of 4 components are nearly absent in severely degraded oils. However, O species with higher DBE values tend to persist in more degraded oils, in which DBE of 5 and 7 are, in general, more abundant in highly biodegraded samples. Note that the PM level 5−10 samples were not included because the O_1 class was not detected in severely biodegraded oils; hence, the MA1 and MA2 parameters can only be used to evaluate biodegradation up to moderate levels.

CONCLUSION

Petroleomics by ESI(−) FT-ICR MS mainly focused on the O_1 and O_2 heteroatom classes proved its usefulness to classify Brazilian oils according to their biodegradation levels, even in a set of oils non-genetically related, with results that generally agreed with the PM biodegradation scale. The A/C ratio showed robustness to assess biodegradation of these Brazilian oils, expanding its broader applicability. A modified SA index that excluded DBE of 1 components was shown to provide better biodegradation estimations. Using the abundances of the O_1 class, two new parameters MA1 and MA2 were proposed and, when used in combination with the A/C ratio, were shown to provide proper biodegradation monitoring.

DOI: 10.1021/acs.energyfuels.7b00109
Energy Fuels 2017, 31, 6649−6657

■ ASSOCIATED CONTENT

Supporting Information

The Supporting Information is available free of charge on the ACS Publications website at DOI: 10.1021/acs.energyfuels.7b00109.

Whole oil chromatograms obtained by GC−FID of the oil samples not presented in Figure 1 (Figures S1 and S2), reconstructed ion chromatograms for the m/z 83 ion obtained by GC−MS (Figures S3−S5), ESI(−) FT-ICR MS spectra of the oil samples not presented in Figure 2 (Figures S6 and S7), and isoabundance contoured plots of DBE versus carbon number (Figure S8) and distribution of DBE relative abundance (Figure S9) both for the O_1 class of selected samples (PDF)

■ AUTHOR INFORMATION

Corresponding Authors

*E-mail: laerciolopesdm@hotmail.com.
*E-mail: geofec@gmail.com.

ORCID

Laercio L. Martins: 0000-0001-6216-990X

Notes

The authors declare no competing financial interest.

■ ACKNOWLEDGMENTS

This work was supported by the Laboratory of Petroleum Engineering and Exploration of the North Fluminense State University (LENEP/UENF) and the Chemistry Institute, University of Campinas (UNICAMP). CENPES/Petrobras also provided the necessary infrastructure to conduct this research, which was funded by PRH20-ANP, Capes, CNPq, and FAPERJ.

■ REFERENCES

(1) Peters, K. E.; Moldowan, J. M. *The Biomarker Guide: Interpreting Molecular Fossils in Petroleum and Ancient Sediments*; Prentice Hall: Englewood Cliffs, NJ, 1993; pp 363.
(2) Peters, K. E.; Moldowan, J. M. *Org. Geochem.* **1991**, *17*, 47−61.
(3) Head, I. M.; Jones, D. M.; Larter, S. R. *Nature* **2003**, *426*, 344−352.
(4) Zhurov, K. O.; Kozhinov, A. N.; Tsybin, Y. O. *Energy Fuels* **2013**, *27*, 2974−2983.
(5) Rodgers, R. P.; McKenna, A. M. *Anal. Chem.* **2011**, *83*, 4665−4687.
(6) Rodgers, R. R.; Schaub, T. M.; Marshall, A. G. *Anal. Chem.* **2005**, *77*, 20 A−27 A.
(7) Marshall, A. G.; Hendrickson, C. L. *Annu. Rev. Anal. Chem.* **2008**, *1*, 579−599.
(8) Robb, D. B.; Covey, T. R.; Bruins, A. P. *Anal. Chem.* **2000**, *72*, 3653−3659.
(9) Kaiser, N. K.; McKenna, A. M.; Savory, J. J.; Hendrickson, C. L.; Marshall, A. G. *Anal. Chem.* **2013**, *85*, 265−272.
(10) Hughey, C. A.; Rodgers, R. P.; Marshall, A. G.; Qian, K.; Robbins, W. K. *Org. Geochem.* **2002**, *33*, 743−759.
(11) Hughey, C. A.; Rodgers, R. P.; Marshall, A. G.; Walters, C. C.; Qian, K.; Mankiewicz, P. *Org. Geochem.* **2004**, *35*, 863−880.
(12) Oldenburg, T. B. P.; Brown, M.; Bennett, B.; Larter, S. R. *Org. Geochem.* **2014**, *75*, 151−168.
(13) Vaz, B. G.; Abdelnur, P. V.; Rocha, W. F. C.; Gomes, A. O.; Pereira, R. C. L. *Energy Fuels* **2013**, *27*, 1873−1880.
(14) Terra, L. A.; Filgueiras, P. R.; Tose, L. V.; Romão, W.; de Souza, D. D.; de Castro, E. V. R.; de Oliveira, M. S. L.; Dias, J. C. M.; Poppi, R. J. *Analyst* **2014**, *139*, 4908−4916.
(15) Corilo, Y. E.; Podgorski, D. C.; McKenna, A. M.; Lemkau, K. L.; Reddy, C. M.; Marshall, A. G.; Rodgers, R. P. *Anal. Chem.* **2013**, *85*, 9064−9069.
(16) Kim, S.; Stanford, L. A.; Rodgers, R. P.; Marshall, A. G.; Walters, C. C.; Qian, K.; Wenger, L. M.; Mankiewicz, P. *Org. Geochem.* **2005**, *36*, 1117−1134.
(17) Hughey, C. A.; Galasso, S. A.; Zumberge, J. E. *Fuel* **2007**, *86*, 758−768.
(18) Liao, Y.; Shi, Q.; Hsu, C. S.; Pan, Y.; Zhang, Y. *Org. Geochem.* **2012**, *47*, 51−65.
(19) Vaz, B. G.; Silva, R. C.; Klitzke, C. F.; Simas, R. C.; Lopes Nascimento, H. D.; Pereira, R. C. L.; Garcia, D. F.; Eberlin, M. N.; Azevedo, D. A. *Energy Fuels* **2013**, *27*, 1277−1284.
(20) Angolini, C. F. F.; Capilla, R.; Marsaioli, A. J. *Energy Fuels* **2015**, *29*, 4886−4892.
(21) Agência Nacional do Petróleo (ANP). *Boletim da Produção de Petróleo e Gás Natural*; ANP: Brasília, Brazil, June 2016; Vol. *70*, pp 1−26.
(22) Nascimento, L. R.; Rebouças, L. M. C.; Koike, L.; Reis, F. A. M.; Soldan, A. L.; Cerqueira, J. R.; Marsaioli, A. J. *Org. Geochem.* **1999**, *30*, 1175−1191.
(23) Milani, E. J.; Araújo, L. M. Recursos Minerais Energético: Petróleo. *Geologia. Tectônica e Recursos Minerais do Brasil*. Companhia de Pesquisa de Recursos Minerais (CPRM): Brasília, Brazil, 2003.
(24) Corilo, Y. E.; Vaz, B. G.; Simas, R. C.; Lopes Nascimento, H. D.; Klitzke, C. F.; Pereira, R. C. L; Bastos, W. L.; Santos Neto, E. V.; Rodgers, R. P.; Eberlin, M. N. *Anal. Chem.* **2010**, *82*, 3990−3996.
(25) Head, I. M.; Larter, S. R.; Gray, N. D.; Sherry, A.; Adams, J. J.; Aitken, C. M.; Jones, D. M.; Rowan, A. K.; Huang, H.; Roling, W. F. M. Hydrocarbon degradation in petroleum reservoir. *Handbook of Hydrocarbon and Lipid Microbiology*; Springer-Verlag: Berlin, Germany, 2010.
(26) Seifert, W. K.; Moldowan, J. M. *Geochim. Cosmochim. Acta* **1979**, *43*, 111−126.
(27) Zhang, D.; Huang, D.; Li, J. *Org. Geochem.* **1988**, *13*, 295−302.
(28) Alves, P. B. Detalhes Sobre a História Geológica da Bacia de Sergipe-Alagoas a partir de Biomarcadores Ácidos e Síntese de Biomarcadores. Ph.D. Thesis, University of Campinas, Campinas, São Paulo, Brazil, 1997.
(29) Silva, A. A. Estudos Geoquímicos com Evidências Paleo-ambientais. maturação e Biodegradação dos Óleos de Diferentes Origens da Bacia Potiguar. Brasil. Síntese de Biomarcadores de Esteróis. Ph.D. Thesis, University of Campinas, Campinas, São Paulo, Brazil, 2008.
(30) Larter, S.; Huang, H.; Adams, J.; Bennett, B.; Snowdon, L. R. *Org. Geochem.* **2012**, *45*, 66−76.
(31) Marshall, A. G.; Rodgers, R. P. *Proc. Natl. Acad. Sci. U. S. A.* **2008**, *105*, 18090−18095.
(32) Meredith, W.; Kelland, S. J.; Jones, D. M. *Org. Geochem.* **2000**, *31*, 1059−1073.
(33) Harwood, C. S.; Burchhardt, G.; Herrmann, H.; Fuchs, G. *FEMS Microbiol Rev.* **1998**, *22*, 439−458.
(34) Wentzel, A.; Ellingsen, T. E.; Kotlar, H. K.; Zotchev, S. B.; Throne-Holst, M. *Appl. Microbiol. Biotechnol.* **2007**, *76*, 1209−1221.

DOI: 10.1021/acs.energyfuels.7b00109
Energy Fuels 2017, 31, 6649−6657